Adhesive bonding and corrosion performance investigated as a function of auminum oide chemistry and adhesives

Abrahami, Shoshan; Hauffman, T.; de Kok, John M.M.; Terryn, Herman; Mol, Arjan

DOI
10.5006/2391

Publication date
2017

Document Version
Accepted author manuscript

Published in
Corrosion: journal of science and engineering

This is an Accepted Author Manuscript of an article published by NACE in the journal Corrosion, available online: https://doi.org/10.5006/2391

Adhesive bonding and corrosion performance investigated as a function of aluminum oxide chemistry and adhesives

Shoshan T. Abrahami *, **, Tom Hauffman ***, John M.M. de Kok ****, Herman Terryn ***, Johannes M.C. Mol **

* Materials innovation institute (M2i), Elektronicaweg 25, 2628 XG, Delft, The Netherlands

** Delft University of Technology, Department of Materials Science and Engineering, Mekelweg 2, 2628 CD, Delft, The Netherlands

*** Department of Materials and Chemistry, Research Group Electrochemical and Surface Engineering (SURF), Vrije Universiteit Brussel, Pleinlaan 2, 1050 Brussels, Belgium

**** Fokker Aerostructures BV, Industrieweg 4, 3351 LB, Papendrecht, The Netherlands

Correspondence to: J.M.C.Mol@tudelft.nl, Delft University of Technology, Department of Materials Science and Engineering, Mekelweg 2, 2628 CD, Delft, The Netherlands.

Abstract

The long-term strength and durability of an adhesive bond is dependent on the stability of the oxide/adhesive interface. As such, changes in the chemistries of the oxide and/or the adhesive are expected to modify its interfacial properties and so to affect the joint performance in practice. The upcoming transition to Cr(VI)-free surface pre-treatments makes it crucial to evaluate how the incorporation of electrolyte-derived sulfate and phosphate anions from, respectively, phosphoric acid- (PAA) and sulfuric acid- (SAA) anodizing are affecting the interfacial chemical properties. Hence, different types of featureless aluminum oxides with well-defined surface chemistries were prepared in this study. The relative amounts of O^{2-}, OH^{-}, PO_4^{3-} and SO_4^{2-} surface species were quantified using X-ray photoelectron spectroscopy (XPS). Next, bonding with two types of commercial aerospace adhesive films was assessed by peel and bondline corrosion tests. The presented results indicate that the durability of the oxide/adhesive interface depends on interplay between oxide and adhesive chemistries. Epoxy adhesion is highly affected by changes in the oxide surface chemistry, especially the amount of surface hydroxyls. However, the performance of anodic oxides with a lower hydroxyl fraction can be significantly enhanced by the presence of covalent bonds using a silane coupling-agent γ-amino propyl triethoxy (APS). On the contrary, results with Redux 775 adhesive exhibit very low sensitivity to variations in the surface chemistry. Bondline corrosion resistance of the joints is mainly determined by the nature of the adhesive, independent of the oxide varying chemistries.

Keywords: Aluminum, aerospace, surface preparation, corrosion resistance, XPS, epoxy, anodizing

1. Introduction

Structural adhesive bonding of aluminum is one of the principal techniques to produce aircraft components [1]. To prepare this type of joint, the aluminum substrate is first subjected to a multi-step pre-treatment. This pre-treatment produces a porous anodic oxide with a thin barrier layer at its bottom, providing the substrate with an increased adhesion and corrosion resistance [2]. In order to preserve its long-term strength, the produced oxide/adhesive interface must retain its properties during a life-long service that includes different mechanical loads, frequent changes in temperature and hostile environments [3].

In the transition to Cr(VI)-free production, aircraft manufacturers are looking to replace chromic acid anodizing (CAA) by alternative electrolytes. Currently, different electrolytes are typically mixed in the anodizing bath to create the conditions that will result in film features similar to CAA anodic oxides. Some examples include boric-sulfuric acid anodizing (BSA)[4], phosphoric acid modified boric-sulfuric and anodizing[5], tartaric-sulfuric acid anodizing (TSA)[6] and phosphoric and sulfuric acid (PSA) anodizing [7]. In this paper, we focus on the latter option being the prime Cr(VI)-free candidate for bonded components that will serve as part of the load-carrying primary aircraft structure.

It is well known that the nature of the electrolyte and the anodizing conditions will affect the oxide properties, such as its morphological features and chemical composition [8, 9]. Different studies have shown that bonding performance is affected by changing the oxide morphology [10-12]. This is often explained by changes in the extent of mechanical interlocking between the oxide and the resin [13]. Changing the anodizing temperature, for example, will significantly affect pore dimensions and general porosity [14]. However, because bond formation (and degradation) is initiated on a molecular level, changes in the chemical properties of the oxide, the type of organic resin and their compatibility are also expected to influence the initial adhesion, as well as its long-term performance [15-17].

One of the main challenges in the study of interfacial adhesion is the detection of interactions at the buried interface. To overcome this limitation and to investigate the type of bondings that are formed, metal oxide interaction with model molecules that represent adhesive functionalities are typically probed. Epoxy adhesive is, for instance, often modeled using different types of amines that are used for epoxy curing [18-20]. Different studies on natural and (electro) chemically grown

oxides have shown that these types of bonding involve relatively weak acid-base interactions [21-24]. On the other hand, a study by Marsh et al [25] showed no specific interaction with epoxypropylphenyl ether itself. As opposed to model molecules, adhesive films undergo curing at elevated temperatures and pressures and typically contain extra additives. In a recent work we demonstrated that bonding between barrier-type anodic aluminum oxides and FM 73 epoxy resin is distorted by water [26]. This was postulated to occur due to the reversible nature of hydrogen bonds that were formed between the oxide and epoxy.

Covalent bonds exhibit much larger bond energy than hydrogen bonds and therefore are much more stable [27]. Numerous studies over the last decades have demonstrated the ability of silanes to form covalent bonds with an aluminum substrate [28-31]. This is achieved using silane molecules that can form an aluminosiloxane (Si-O-Al) bond [32]. Upon curing, excessive molecules will condense among themselves, forming Si-O-Si bonds. By the right selection of the molecule chemical functionalities, silane films can be used as coupling agents, linking between organic and inorganic materials and produce a thick corrosion-resistant coating [33]. Since the Al-O-Si bond can be hydrolyzed, coating durability will be determined by the extent of cross-linking and subsequent barrier properties to the diffusion of water. Furthermore, using an amino silane like γ-amino propyl triethoxy (APS) enables an additional interaction with epoxy. While the silane groups can form covalent bonds with the substrate, the amino group is able to act as an additional hardener for the epoxy matrix [25]. This type of silanes are called coupling agents for this double functionality [34]. Since silanes react with metals via their OH groups, maximizing the amount of these groups at the oxide surface is desired. In a study by Franquet et al. [35], it was shown that a pre-treatment increasing the amount of surface hydroxyls will in turn result in silane films of better uniformity and larger thickness.

This study investigates how changes in the oxide chemistry influence adhesion with two types of commercial aerospace resins: FM 73 and Redux 775, an epoxy and vinyl phenolic adhesives, respectively [3]. To exclude the contribution of mechanical interlocking, anodic oxide growth was stopped during the formation of the barrier layer, producing relatively thin and featureless oxides [7]. Since the hydroxyl fraction is expected to play a crucial role in bonding with aluminum oxides, the classic alkaline and boiling water pre-treatments that produce the highest amount of surface

hydroxyls [36] are included for comparison. To examine the different types of interfacial bonding, APS silane was applied on some of the epoxy test panels.

2. Materials and Methods

Two types of specimens were used in this study. Model (laboratory) specimens were used for surface characterization. These specimens were electropolished to produce a mirror-like smooth surface that is suitable for quantification purposes. Industrial test specimens were used for floating roller peel. To make sure that featureless barrier-type layers are formed, anodizing is stopped at the end of the linear increase with time [37], as found by preliminary tests [26]. Both preparation methods are detailed below.

2.1 Model Specimens for XPS Analysis

Samples were cut from a 0.3 mm thick sheet of commercially pure aluminum (99.99 %, Hydro). To remove the surface oxide and the modified surface layers that are present on the surface in its as-received state, as well as providing a flat substrate for analysis purposes, specimens were first electropolished. This was done after the substrate was etched in an aqueous solution of 25 g/l NaOH at 70°C for 1 minute, followed by rinsing for 15 s with deionized water and then ultrasonically rinsed for 3 additional minutes. The substrate was then electropolished for 6 min in a solution of 80 vol.% (absolute) ethanol and 20 vol.% perchloric acid, at a current density of 70 mA/cm^2 and 10°C. Subsequently, it was rinsed following the same procedure, dried with compressed air and stored in a sealed plastic bag. Later, each sample was given one of the anodizing pre-treatments listed in Table 1.

Table 1: Summary of the electrolyte composition for the different surface pre-treatments.

Abbreviation	Pre-treatment	Electrolyte composition
PAA	Phosphoric Acid Anodizing	25 g/l H_3PO_4
SAA	Sulphuric Acid Anodizing	*10g/l H_2SO_4
CAA	Chromic Acid Anodizing	40g/l CrO_3
Alkaline	Alkaline immersion	25g/l NaOH, 30s, RT
Hydrothermal	Boiling water immersion	Boling (demi-)water, 30s

* 5g/l was used for the preparation of the floating roller peel specimens instead.

Galvanostatic anodizing at 10 mA/cm^2 for 4 s was performed with SM120-25 power-supply unit (Delta Elektronika) equipped with an Ethernet interface connection to monitor the cell voltage. Model specimens were anodized in a three-electrode cell filled with 400 ml solution and two AA1050 aluminum cathodes. After each of the described pre-treatments, the substrate was again thoroughly rinsed as previously described. Anodizing conditions were preselected to yield featureless anodic oxides by stopping the oxide growth at the end of the region in which the voltage was increasing linearly with time, the part which is associated with the formation of the barrier layer [37]. In order to limit atmospheric contamination, samples were placed in the pre-vacuum chamber for analysis no longer than 10 minutes after the pre-treatment was completed.

2.2 Panels for Floating Roller Peel Test

For practical reasons, peel tests following aerospace protocol could not be made with the soft pure aluminum that was used for surface characterization. Therefore, AA2024-T3 alclad (clad layer AA1230) aluminum test sheets of 250x95x1.6 mm and 300x95x0.5 mm were used for the thick and thin panels, respectively. Before anodizing specimens were degreased, alkaline etched and desmutted. Degreasing was achieved by wiping the panels with ethanol. This was followed by a 2 min. alkaline etching with 40 g/L P3 Almeco 51 (from Henkel) at 35°C and a 1 min. pickling with 35 vol.% HNO_3 at RT. After each step, the panel was thoroughly rinsed with running demineralized water (at room temperature, ±22°C), followed by 1 min. immersion rinsing in an agitated beaker of fresh demineralized water. Then the panels were anodized in one of the electrolytes listed in Table 1. Anodizing at constant current density of 5 mA/cm^2 was performed for 8 s. Although the applied current density is lower than for the model specimens, the anodizing time is doubled so that the total amount of current passing is the same. After anodizing, the panels were rinsed and dried with compressed air. The panels were then bonded (without primer) with one of the selected adhesives, no longer than 10 minutes after the pre-treatment of the thin panel was completed. After bonding, the panels were stored in a sealed plastic bag for up to 24 hours before curing. Curing following the manufacturer instructions was performed using a Joos hot plate press. FM 73 curing was achieved at 6 bar and 120°C for 75

minutes. Redux 775 was cured at 9.9 bar and 155°C for 45 minutes. Measured adhesive thickness (after curing) corresponds to 0.1 ± 0.2 mm for FM 73 epoxy and 0.2 ± 0.2 mm for Redux 775. Silane layers were applied on some panels before FM 73 epoxy adhesive application. The addition of silanes did not affect the adhesive film thickness, as measured after curing.

2.3 Adhesives Chemistries

Redux 775 and FM 73 are two typical aerospace structural adhesives. Redux 775 (Hexcel) is a vinyl phenolic resin. It is the first man-made adhesive that was used to bond aircraft structures [1]. The general building blocks of Redux are shown in Figure 1. Its most basic unit is the phenol molecule (Figure 1 (a)). A resole phenolic resin (Figure 1 (c)) is produced by the reaction between phenol and formaldehyde (in excess, Figure 1 (b)) using a basic catalyst [38]. Because phenolic resins are brittle, polyvinyl formal (PVF, Figure 1 (d)) is added to improve the fracture toughness. PVF is made by acidic reaction between poly(vinyl alcohol) (PVA) and formaldehyde. The poly(vinyl alcohol) is, in turn, made by hydrolysis of polyvinyl acetate. Thus, residual alcohol and ester functionalities are usually present in PVF, as indicated in Fig, 1 (d). Phenolic adhesive provides a large amount of active sites on the phenol ring and residual hydroxyl methyl groups that enable its self-curing. Alternatively, it can condense with the phenolic hydroxyl of the residual hydroxyls of the PVA [3]. As a result, the adhesive can develop a high level of cross-linking.

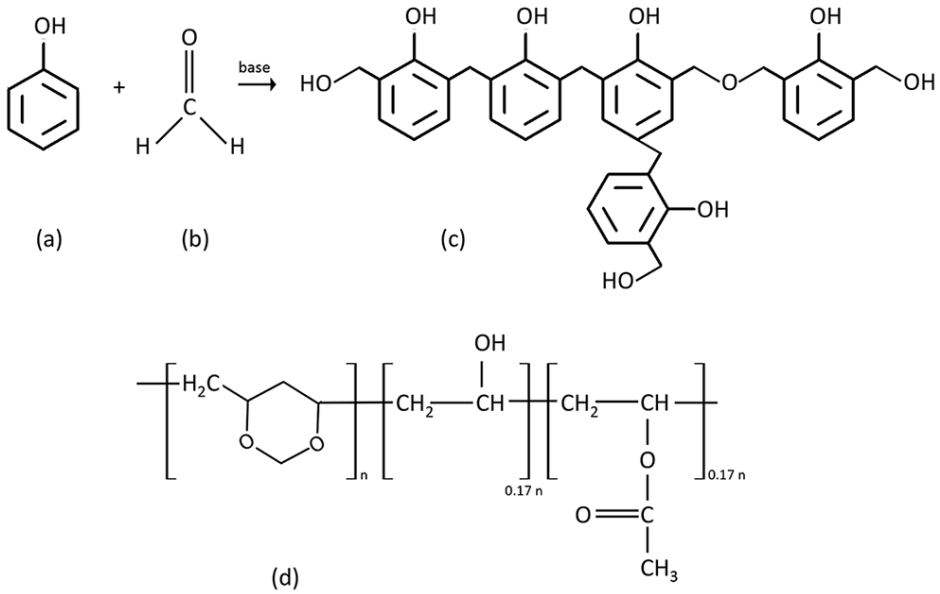

Figure 1: Molecular structure of the basic components of Redux 775 resin:(a) phenol, (b) formaldehyde, (c) a phenolic resole product and (d) formaldehyde polyvinyl formal (PVF, left) containing trace amounts (typically 0.1 to 0.17) of poly(vinyl alcohol), and poly(vinyl acetate).

FM 73 (Cytec Engineering Materials) is a typical epoxy structural adhesive that does not contain silanes. It is based on a DGEBPA (diglycidyl ether of bisphenol A, Figure 2 (a)). The epoxide ring in DGEBPA is the reactive moiety in this molecule and, hence, a schematic representation of epoxy curing is shown in Figure 2 (b). The reaction proceeds by ring opening, which typically occurs by an amine addition [25, 39].

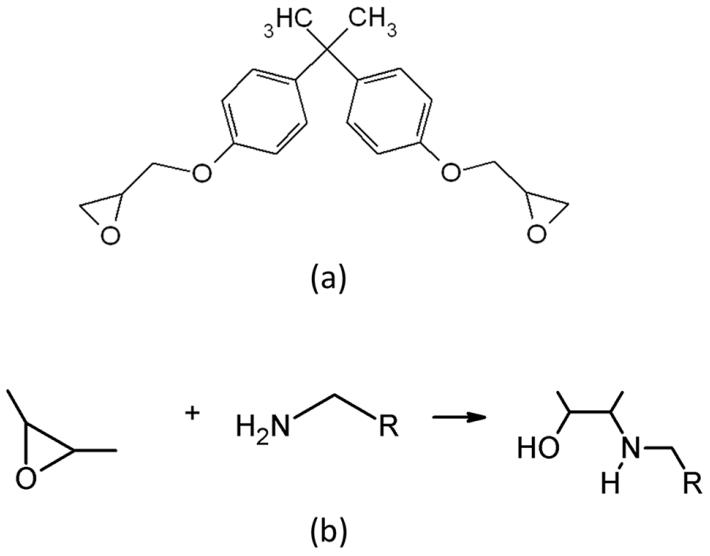

Figure 2: Molecular structure of DGEBPA (diglycidyl ether of bisphenol-A), (a) and representative reaction of epoxide ring opening reaction using an amine curing-agent, (b).

2.4 Silane Application

The silane applied in this study is γ-amino propyl triethoxy (APS), which is an amino silane with the molecular structure given in Figure 3. Before its application the silane was hydrolyzed for 24 hours under continuous (magnetic) stirring. During this process the ethyl groups are converted to silanol (-SiOH) groups that can react with the aluminum. This was accomplished in a mixture of 2 vol.% APS in (distilled) water at pH 9 (adjusted with acetic acid).

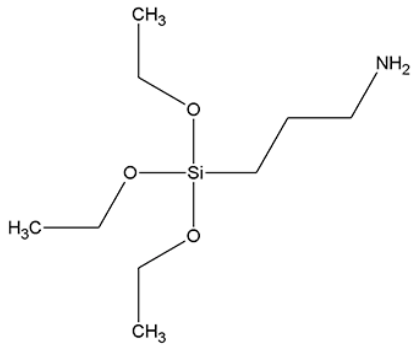

Figure 3: Molecular structure of APS.

After 24 hours, the mixture was ready and part of it was diluted to prepare a second mixture of 0.5 vol.% APS. For each concentration, a solution of pH 5.7 and pH 9 were made using acetic acid (when needed). Directly after the anodized panels were rinsed, silanes were applied from the solution by dipping the panels for 30 s. Thereafter, the panels where air-blown dried and bonded with FM 73 epoxy. Silane-treated panels for floating roller peel tests were further prepared following the description in section 2.2.

2.5 Analysis Methods

2.5.1 X-Ray Photoelectron Spectroscopy (XPS)

XPS spectra were collected using a PHI5600 photoelectron spectrometer (Physical Electronics) with an Al *Kα* monochromatic X-ray source (1486.71 eV of photons). The vacuum in the analysis chamber was approximately $5x10^{-9}$ Torr during measurements. The full elemental composition was initially determined by acquiring survey spectra on a spot size of 0.8 mm in diameter recorded in the full range (0–1400 eV) at analyzer pass energy of 187.85 eV and step size 0.5 eV. High-resolution scans of aluminum (Al 2p), oxygen (O 1s), carbon (C 1s), phosphorus (P 1s) and sulfur (S 2p) photopeaks were recorded using pass energy of 23.5 eV and step size 0.1 eV. Measurements were performed at takeoff angles of 45° and 15° with respect to the sample surface. The reproducibility of the measurements was verified by (at least) two repetitions.

XPS data was analyzed using PHI Multipak software (V9.5.0.8). Before curve fitting, the energy scale of the spectra was calibrated relative to the binding energy of adventitious hydrocarbons in

the C1s peak at 284.8 eV. Curve fitting was done after a Shirley-type background removal, using mixed Gaussian (80–100%) – Lorentzian shapes.

2.5.2 Mechanical Testing

Floating roller peel tests were executed according to ASTM D3167 - 03a [40]. Of each bonded panel, three strips of 25x250 mm were cut with a diamond saw. After fixing the test strips in the apparatus, the unbound end of the specimen was attached to the lower head of the testing machine. The thin aluminum panel was then peeled off the thick panel with a speed of 100 mm/min while the peeling load versus head movement (or load versus distance peeled) was recorded. All tests were performed at ambient temperature. The first half of the specimen was peeled under dry conditions. Water with surfactants (Extran MA 02 neutral, Merck) was then injected at the crack-tip while peeling the second half of the panel. The presence of surfactants ensures that the water will reach the interface at the crack tip in order to test its stability under wet conditions.

2.5.3 Bondline Corrosion Tests

Additional specimens were placed in the salt spray cabinet for environmental exposure tests at Fokker Aerostructures. The corrosive environment used in the test is a 5% NaCl in distilled water at 35°C (ISO 9227). One specimen was used for each type of pre-treatment and exposure period. After 1, 2 and 4 weeks specimens were taken out. It was then subjected to a dry floating roller peel test and visually inspected for bondline corrosion.

3. Results and Discussion

3.1 Oxide Chemical Characterization

The surface chemistry of model panels was characterized by angle-resolved XPS measurements. Before recording each high-resolution spectrum, a survey scan was taken. An example for a survey spectrum of the different oxides is shown in Figure 4. The main elements detected in all oxides are oxygen, aluminum and carbon. Carbon is the only element that is not an integral part of the anodic oxide. It arises from ambient contamination during sample processing. The amount of carbon on each sample varied somewhat according to handling procedure and processing time. Generally, however, carbon contamination on the hydrothermal specimens was much lower than

on the other samples. Phosphor and sulfur were detected in the oxides that were prepared in phosphoric and sulfuric acids (Figure 4 (a) and (b), respectively). Smaller amounts (almost negligible, hence not visible in the survey spectra in Figure 4 (c)) of chromium were detected on CAA samples. These observations are in agreement with earlier literature [41].

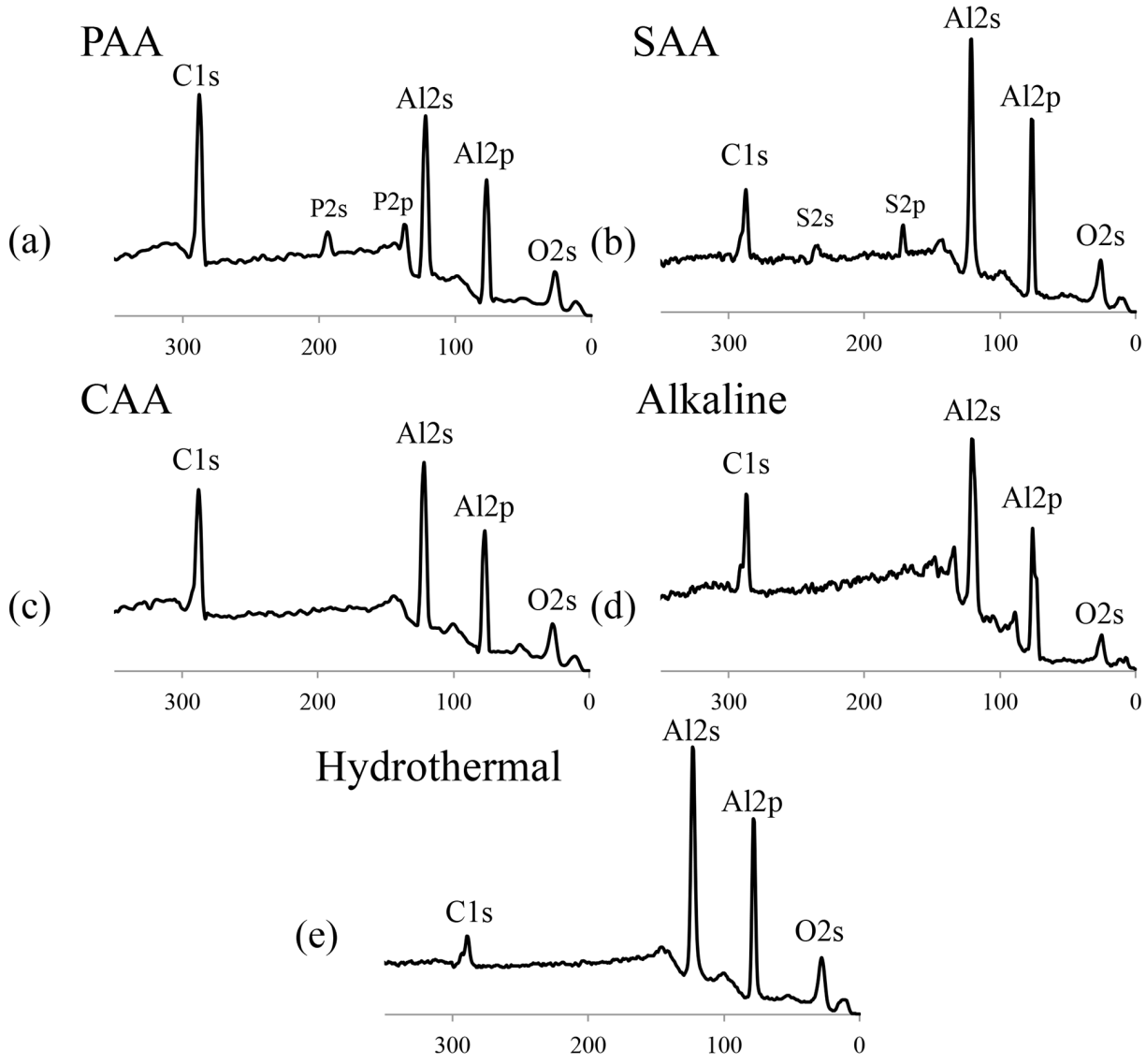

Figure 4: Relevant sections of the XPS survey spectra (0-350 eV) measured on the different oxides.

To link surface chemistry to bonding performance, the different surface species at the surface of the different oxides were quantified. This has already been completed for PAA, SAA and CAA in

our previous publication [26]. These results are included in here, along with the quantification of the hydroxyl percentage on alkaline and hydrothermal treatments. Therefore, a short description of the analysis method is outlined in here: high-resolution spectra of O1s, C1s, Al2p, S2p and P2s were measured. The data was fitted to resolve the CO-, COO-, PO_4^{3-}, SO_4^{2-}, OH^- and O^{2-} components using the constraint parameters that are provided in Abrahami et al. [26]. The fitted intensity areas were then used to find a solution for the concentration of the different surface species, while taking into account overlapping in the binding energy of different components in the O1s photopeak. Next, the relative amounts of O^{2-}, OH^-, PO_4^{3-} and SO_4^{2-} (in %) were determined by the ratio, as presented in Equation 1 for OH^-.

$$OH^-(\%) = \frac{C_{OH^-}}{C_{OH^-} + C_{O^{2-}} + (4 \times C_{PO_4^{3-}}) + (4 \times C_{SO_4^{2-}})} \times 100 \qquad \text{Eq. 1}$$

Results are summarized in Figure 5, for takeoff angles of θ =15° and 45°. Calculations show that anodizing in PAA and SAA electrolytes modifies the anodic oxide chemistry by the incorporation of electrolyte-derived phosphate and sulfate anions. As a result, PAA and SAA oxides exhibit a much lower hydroxyl fraction compared to CAA. Since phosphate incorporation is the highest in the group, PAA oxide has the lowest surface OH fraction, followed by SAA and CAA. This trend is valid for both anodizing temperatures. As expected, oxides prepared by alkaline and hydrothermal treatments exhibited the highest hydroxyl percentage, between 40 and 50%, in accordance with previous studies [22, 36].

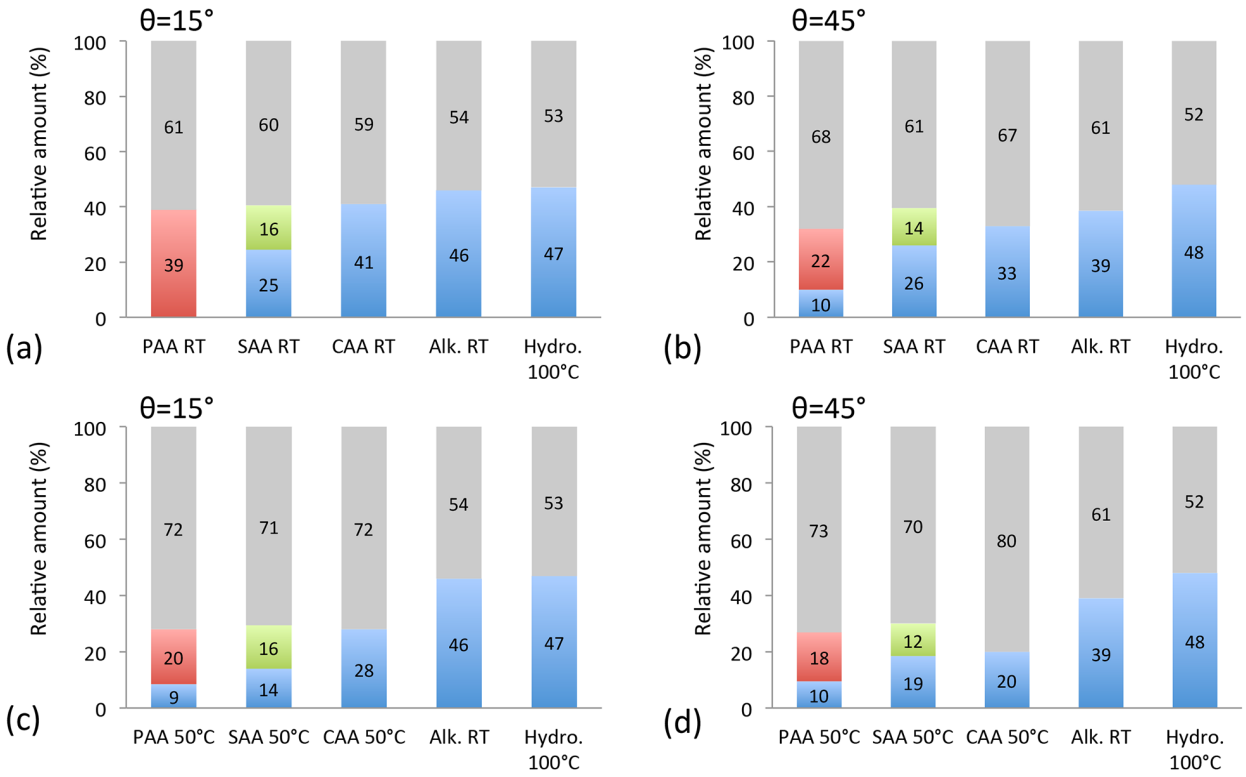

Figure 5: Calculated relative amounts of O^{2-} (grey), OH^- (blue), PO_4^{3-} (red) and SO_4^{2-} (green) on the different pretreated specimens anodized at room temperature (RT) (a) and (b) and 50°C (c) and (d). Additional non-anodizing treatments, alkaline and hydrothermal (hydro), are added next to RT and 50°C respectively.

Variations in the takeoff angle, θ, represent a different amount of detected volume under the surface. Since the interaction depth of the grazing angle of θ =15° is much lower than for θ =45°, it provides a rough indication for the in-depth distribution of the species within the oxide. The higher phosphate concentration at θ=15° indicates of a higher concentration in the top surface layers. Conversely, sulfur concentration is relatively constant in both measurements. These observations are in agreement with earlier in-depth study performed using Auger electron spectroscopy (AES) [7]. As oxide hydration is mostly dominant close to the surface, oxides other than SAA and PAA exhibit a higher hydroxyl fraction at θ =15° [42, 43].

3.2 The Effect of Oxide Chemistry on Bonding with Different Adhesives

3.2.1 Phenol-Base Adhesive (Redux 775)

To measure the quality of bonding as a result from adsorptive interactions, peel tests were carried out with barrier-type oxides bonded with Redux 775. Strength results are displayed in Figure 6, as a function of the hydroxyl percentage at the surface (θ =15°). Results are divided into anodic oxides prepared at room temperature (Figure 6 (a)) and at 50°C (Figure 6 (b)), with alkaline (prepared at room temperature) and hydrothermal (boiling water) treatments shown in both figures. As seen in Figure 6, peel strengths are generally very low and show no particular trend in relation to the calculated amount of hydroxyls. Both dry (empty markers) and wet (filled markers) peel strengths seem to be independent of the pre-treatments and the anodizing temperature. Images of representative open joint are shown in Figure 7. A thin layer of adhesive is visible on top of the thin aluminum panel, hence, failure appears to occur at or just adjacent to the oxide/ adhesive interface. Also, no distinction is seen between the part in the panel that was tested under dry- and wet conditions.

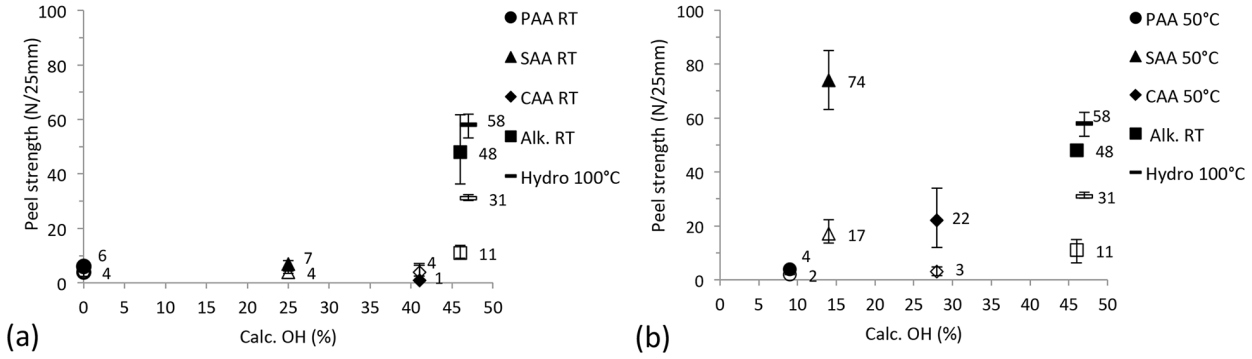

Figure 6: The average dry (empty markers) and wet (filled markers) peel strength vs. the calculated hydroxyl percentage (θ=15°) on barrier-type oxides for anodizing at RT (a) and 50°C (b) and adhesively bonded with Redux 775 phenolic adhesive (no primer). The error markers represent the minimum and maximum measured values.

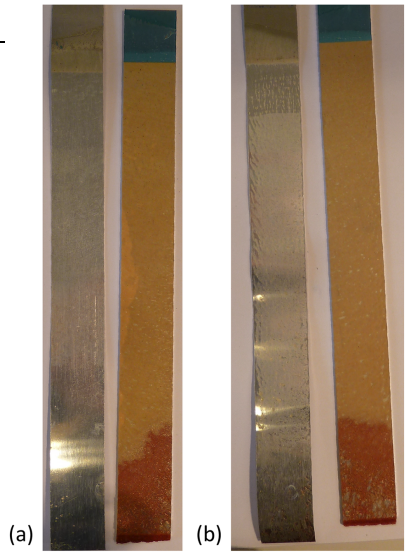

Figure 7: Visual images of peeled panels bonded with Redux 775 after PAA RT (a) and PAA 50°C (b). The peeled area starting a few centimeters below the blue tape was first peeled under dry- and then wet conditions.

Redux is a high-strength adhesive and it appears that the applied changes in the surface chemistry are not sufficient to induce variations in the adhesion strength across the various surface treatments due to relatively strong adsorptive interactions in all cases. Nevertheless, the wet peel strength of most oxides is slightly higher than their corresponding dry peel strength. In case of good adhesion and cohesive fracture in the adhesive, a slight increase in peel values measured in the presence of water during tests with porous industrial oxides. Due to the water the mechanical properties of the adhesive can change, with lower yield stress and increased toughness. This behavior is typically assigned to toughening of the resin in the presence of water.

Considering the chemical composition of Redux 775, adsorption to all substrates via alcohol and phenol groups present on the phenolic resole product can be expected according to our previous studies using model molecules [24]. In this study, the highest peel strengths were achieved with the hydrothermal, alkaline and CAA oxides. These are the same oxides that were formerly found to adsorb phenol molecules better than the other oxides, presumably due to the availability of weaker basic hydroxyl groups. Hence, the slight increase in peel strength after the transition from dry- to wet peel in here may be related to increased interfacial interactions in the presence of the weakly acidic phenols that are leached out of the resin in the presence of water to temporarily stabilize the interface [44] (since, as found earlier in Abrahami et al. [24], these reactions are

reversible). This behavior has also been observed with other polymers including a study with poly(methyl methacrylate) (PMMA) polymer, Tannebaum et al.[45] found that water helps to mediate bonding. Similar observations were recently reported by Pletincx et al.[46] using in-situ measurements, showing that water can stabilize the formation of carboxylate bonds on native aluminum oxides.

3.2.2 Epoxy-Based Adhesive (FM 73)

Similar tests were performed with an epoxy adhesive, FM 73. Peel measurements with anodic oxides were reported previously [26]. The results in here (Figure 8) compare the performance of anodic oxide versus simple chemical treatments in alkaline solution and boiling water (hydrothermal). As opposed to the previous results with Redux, the dry peel strength measured with epoxy is relatively high. The dry peel strength does not show a clear increase with the amount of hydroxyls (hence, to the type of anodizing electrolyte). Wet peel strength (filled markers in 8), on the other hand, linearly increases with the percentage of surface hydroxyls. This dependence indicates that bonding is established via the hydroxyl groups at the surface. Additionally for the anodic oxides, wet peel strength increases with the anodizing temperature.

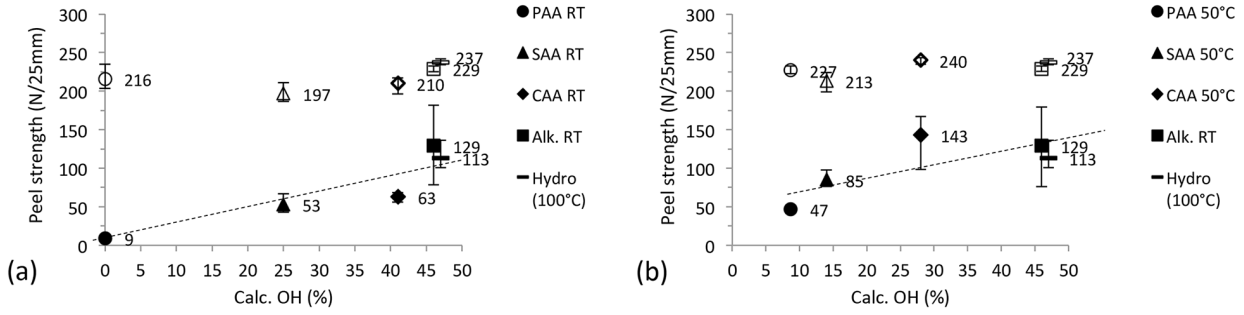

Figure 8: The average dry (empty markers) and wet (filled markers) peel strength vs. the calculated hydroxyl percentage at the surface (θ=15°) on barrier-type oxides for anodizing at RT (a) and 50°C (b) and adhesively bonded with FM 73 epoxy adhesive (no primer). The error markers represent the minimum and maximum measured values.

It is interesting to note that in this case the dry peel strength of all oxides, excluding the hydrothermal oxide, is much higher than the wet peel strength. Visual inspection of the peeled

panels in Figure 9 indicates that two different modes of failure occurred. Mainly cohesive failure occurred within the adhesive during dry peel. The adhesive is visible on both sides of the joint. Under wet conditions, the failure mode changes from cohesive to interface failure. This behavior was observed in all the tested panels, regardless of the measured wet peel strength. This indicates that interfacial interactions are stronger than the cohesive strength of the adhesive under dry conditions. Upon the ingress of water, the stability of the interface is the critical factor. It appears that water entering the interface between oxide and epoxy causes disbonding and the adhesion strength is reduced by a factor of at least two. These experimental measurements confirm previous predictions made by modeling the interface using density functional theory (DFT) calculations. Semoto et al. [47] have found that the main contribution to adhesion between epoxy and aluminum oxide originates from a network of hydrogen bonds with surface hydroxyls. Hence, the larger amount of hydroxyl groups available for interactions, the denser and stronger the resulting interfacial bonding. Other studies that apply molecular and atomic simulations also predict disbonding and adhesion reduction in the presence of water molecules at the interface [48-50]. These predictions are also confirmed by the results showing interface failure and significant reduction in strengths of FM 73 epoxy joints peeled under wet conditions. In the absence of surface roughness that can retard interfacial diffusion of water, bonds stability is crucial for a durable adhesion.

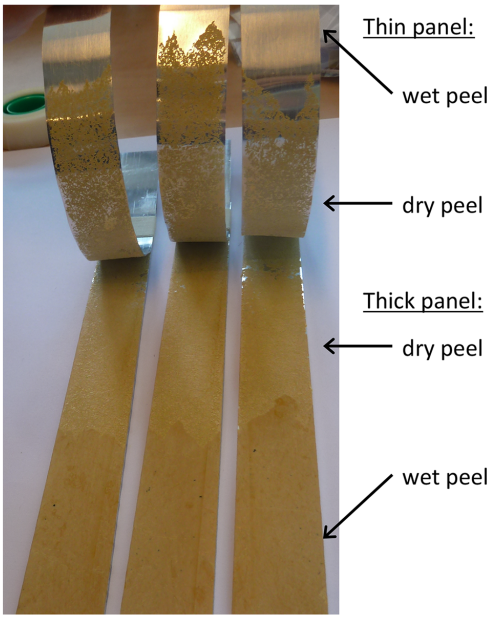

Figure 9: Visual impression of typical peeled panels (CAA RT) bonded with FM 73 epoxy. Dry conditions lead to cohesive failure, with the adhesive seen on both sides of the panels and interface failure under wet conditions, in which the substrate is revealed on the thin panel and an intact adhesive on the other panel (dark yellow).

3.3 Silane Effect on Adhesion

Results in the previous section indicate that adsorptive interactions between aluminum oxide and FM 73 epoxy are not stable under wet conditions. It is therefore of great interest to find out if interfacial stability and durability using only adsorptive adhesion mechanism can be increased by the presence of covalent bonds. Similar to epoxy, silanes first adsorb onto the aluminum surface through hydrogen bonds. Upon curing, hydrogen bonds are replaced by the covalent Al-O-Si bonds. To this aim two types of oxides, CAA and PAA, were studied. These two anodic oxides present the best and worst mechanical performance, respectively, as shown in Figure 8. A summary of the peel test results after silane post-treatments of PAA and CAA is listed in Table 2. For comparison, tests with barrier- and porous oxides without a silane layer (no primer) were also included. Results in Table 2 confirm that the interface stability under wet conditions is generally increased by the formation of covalent bonds (with one exception, measured after CAA 2 vol.% APS post-treatment). It is, however, interesting to note that dry adhesion after PAA silane treatment remains similar, while the dry peel of CAA oxides after silane post-treatment is worse than before.

Table 2: Average peel strength (of 3 repetitions) after silane post-treatment with FM 73 epoxy adhesive. Failure mode: C = cohesive, I = interface.

	Oxide type	Silane conditions	Dry peel (N/25mm)	Failure Mode	Wet peel (N/25mm)	Failure Mode
PAA, RT	Barrier	-	216 ± 14	C	9 ± 1	I
	Barrier	2 vol.%, pH 5.7	214 ± 10	C	208 ± 8	I
	Barrier	0.5 vol.%, pH 5.7	232 ± 9	C	60± 15	I
	Barrier	2 vol.%, pH 9	227 ± 7	C	92 ± 26	C/I
	Barrier	0.5 vol.%, pH 9	208 ± 5	C	18 ± 4	C/I
	Porous*	-	200± 10	C	262± 6	C
CAA, RT	Barrier	-	243 ± 9	C	88 ± 6	I
	Barrier	2 vol.%, pH 5.7	177 ± 23	C	225 ± 1	C
	Barrier	0.5 vol.%, pH 5.7	172 ± 13	C	227± 7	C

Barrier	2 vol.%, pH 9	155 ± 27	C	83± 6	C/I
Barrier	0.5 vol.%, pH 9	124 ± 20	C	203± 2	C
Porous **	-	236 ± 4	C	244± 7	C

* Porous PAA was prepared by anodizing for 20 min. at 18V, ** Porous CAA was prepared by anodizing for 40 min. following the 40/50V scheme [11].

3.3.1 Solution pH Effect on Bonding

The deposited silane layers generally improve the wet adhesion of all barrier oxides bonded with epoxy. Both PAA and CAA oxides show the most pronounced improvements after treatment of 2 vol.% at lower pH of 5.7. In these cases, the wet adhesion approaches the value measured for the porous oxides (Table 2). The natural pH of APS is 10.5 [51]. At pH 5.7, the silanol groups are negatively charged (Si-OH → Si-O$^-$) [51] and are, therefore, expected to readily react with a positively charged surface hydroxyls. The solution pH will also affect the charge of the Alumina surface, as indicated by the zeta potential [52]. A zero zeta potential is called the isoelectric point (IEP), which is the point where the substrate is not charged. The isoelectric point of natural aluminum oxide is about 8.7. As a consequence, the silane solution at pH below this value is expected to carry a net positive charge that will support the formation of silanol bonds more than at pH 9.

3.3.2 Silane Concentration Effect on Bonding

Besides adhesion promotion through the formation of covalent bonds, the application of silanes was found to improve the overall durability of the interface through the formation of a highly cross-linked network [34]. This can only take place in the presence of excessive silanol groups. Upon curing, non-reacted neighboring silanol groups can condensate to form siloxane (Si-O-Si) bonds. Hence, a higher silane concentration will enable the formation of thicker layers that will allow for a higher cross-linking density.

Two different concentrations of silane solutions were applied: 0.5 and 2 vol.%. Since the present goal is to improve adhesion, the chosen concentrations are relatively low and were found to have no effect on the total thickness of the adhesive as measured after curing (section 2.2). Although the 2 vol.% is expected to provide better results, due to the presence of more excessive silanol groups, there is no significant effect of the concentration within this range.

3.4 Bondline Corrosion

Bondline corrosion tests were performed for anodizing at room temperature and for alkaline (RT) and hydrothermal (100 °C) treatments. A summary of the results is listed in Table 3, along with the values and standard deviation of the same treatments pre-SST. Images of the demonstrative panels are shown in Figure 10 and 11. Except for the hydrothermal oxide (both adhesives) and alkaline treatments (only Redux 775), all other joint bonded with FM 73 epoxy already failed after 1 week in the salt spray cabinet and could be easily opened by hand (represented by the – sign in Table 3). Visual inspection of the panels revealed extended corrosion on both sides of the joint (for example, see Figure 11 (a)), showing white precipitates on both sides of the panel (visible on the thin panel side and under the adhesive). Similar observations were made after two and four weeks of testing.

Table 3 Summary of peel test results after different exposure periods in the salt spray cabinet. All tests were performed after room temperature anodizing in PAA, SAA and CAA (the - sign means that the joint was opened by hand). (Dry) peel strength values pre-SST are the average values measured from three different panels. Values measured after SST are from one tested panel.

			Peel strength (N/25mm)			
Adhesive	Treatment	Pre-SST	St. dev.	1 week SST	2 weeks SST	4 weeks SST
Redux 775	NaOH	11	2	13	10	-
	Hydro.	31	4	43	28	-
	PAA	4	2	4	-	-
	SAA	4	0	12	-	-
	CAA	4	2	-	-	-
FM 73	NaOH	229	4	-	-	-
	Hydro.	237	5	252	148	-

	PAA	216	16	-	-	-
	SAA	197	12	-	-	-
	CAA	210	12	-	-	-

An image of the hydrothermal oxide bonded with FM73 epoxy is shown in Figure 10 (a) after 1, 2 and 4 weeks in the salt spray cabinet. Corrosion starts from the edges of the panels and is already visible as white precipitates after 1 week, but it is then limited to 2-3 mm from the edge (mostly at the bottom part). The peel strength is still high and at the same level as the average measured pre-SST. After two weeks in the salt spray cabinet, corrosion marks protrude for about 5-10 mm from the bottom and side edges of the panel. The corresponding peel strength is then also drastically lower (reduced by 41 percent). After four weeks, corrosion is covering a substantial part of the (thick) panel and the joint can be easily opened by hand.

In Figure 10 (b), the corresponding images of hydrothermally treated panels bonded with Redux 775 are shown. After one and two weeks in the salt spray cabinet, the measured peel values are in the same order of magnitude as the values measured pre-SST (Table 3). In this case, it appears that failure still occurs as a result of de-adhesion at the interface rather than corrosion failure. After four weeks the panel can be opened by hand, but there is still no sign of corrosion. These results indicate that susceptibility to corrosion is very closely related to interface chemistry which in this case is determined by the chemistry of the adhesive.

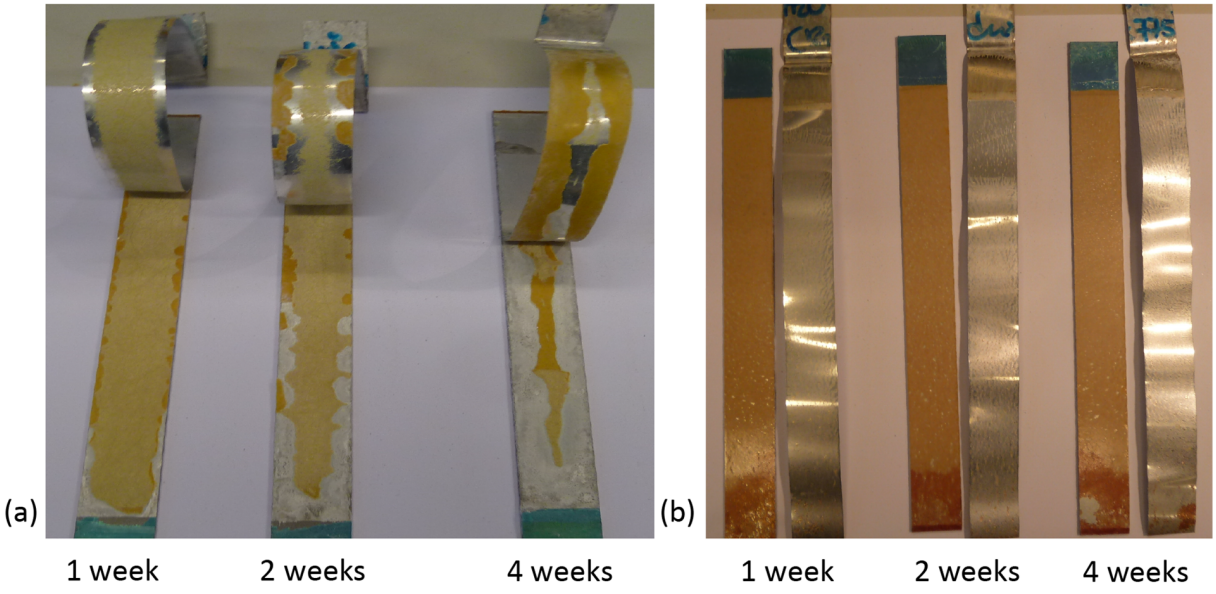

Figure 10: Macroscopic images of the peeled panels after various periods in the salt spray cabinet. Panels received hydrothermal pre-treatment with FM 73 (a) and Redux 775 adhesives (b), without any primer.

Except for the hydrothermal, all the other panels exhibited similar trends. There was clear distinction in the corrosion resistance of FM 73 and Redux 775 (e.g. in Figure 11 (a) and (b), respectively). All FM 73 panels exhibit extensive corrosion while little to no corrosion has been observed on panels bonded with Redux 775. Although the bond strength of joint prepared with Redux 775 is substantially lower than for FM 73, the measured low peel strength is due interfacial failure since these are no signs of corrosion.

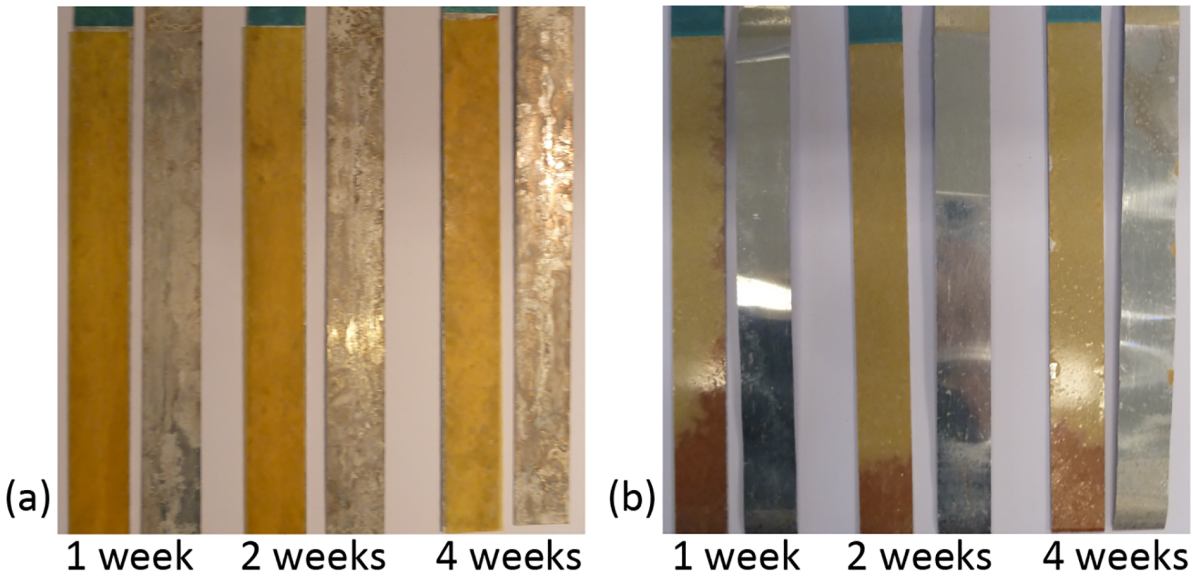

Figure 11: Macroscopic images of the SAA peeled panels after various periods in the salt spray cabinet: bonded with FM 73(a) and Redux 775(b).

Since components of the adhesive can leach out in an aqueous environment, the interface formed with Redux retain the weakly acidic character of the phenol, which stabilizes the aluminum oxide against hydration [44]. This type of behavior is, according to Brockmann et al. [44], one of the main reasons of its prolonged industrial application, providing excellent protection against corrosive degradation. In contrast, the alkaline environment that is formed by epoxies results in high susceptibility to bondline corrosion and leads to the attack of the aluminum oxide [44]. Consequently, it is advised by the manufacturer to combine FM 73 with a corrosion inhibiting primer (typically BR 127).

4. Conclusions

This study compared the performance of oxides with ranging surface chemistries bonded with two types of aerospace adhesives: FM 73 epoxy and Redux 775. In the absence of surface features, mechanical peel tests measure the adhesion strength as a result of adsorptive interactions between the two phases. The presented results indicate that the formation, as well as the durability, of the oxide/adhesive interface depends on interplay between oxide and adhesive chemistries. Based on the results, the following conclusions emerge:

- Interface bonding and stability is influenced by oxide- and adhesive chemistries.
- Interfacial bonding with both FM73 epoxy and Redux 775 appears to be based on relatively weak molecular interactions.
- Maximizing the amount of surface hydroxyls is favorable for bonding with FM 73 epoxy adhesive. It follows from experimental observations that this is due to a higher binding density with surface hydroxyls.
- Results generally confirm that the presence of covalent bonds, provided by a silane-coupling agent, improves the stability of the interface under wet conditions.
- Bondline corrosion resistance is determined by the nature of the adhesive, independent of the oxide chemistries investigated in here.

5. Acknowledgements

This research was carried out under the project number M11.6.12473 in the framework of the Research Program of the Materials innovation institute M2i (www.m2i.nl).

6. References

1. A. Higgins, *Int. J. Adhes. Adhes.* 20, 5 (2000): p. 367-376.

2. G.E. Thompson, *Thin Solid Films* 297, 1–2 (1997): p. 192-201.

3. J. Bishopp, in *Adhesives for Aerospace Structures*, ed. S. Ebnesajjad, ed.(Oxford: William Andrew Publishing, 2011), p. 301-344.

4. BAC 5632, "Process Spec. Boric Acid -- Sulfuric Acid Anodizing, Revision D" Boeing, 2004), p.

5. J.-s. Zhang, X.-h. Zhao, Y. Zuo, J.-p. Xiong, *Surf. Coat. Technol.* 202, 14 (2008): p. 3149-3156.

6. M. Curioni, P. Skeldon, E. Koroleva, G.E. Thompson, J. Ferguson, *J. Electrochem. Soc.* 156, 4 (2009): p. C147-C153.

7. S.T. Abrahami, T. Hauffman, J.M.M. de Kok, J.M.C. Mol, H. Terryn, *J. Phys. Chem. C* 119, 34 (2015): p. 19967-19975.

8. G.D. Sulka, in *Highly Ordered Anodic Porous Alumina Formation by Self-Organized Anodizing*, ed.Wiley-VCH Verlag GmbH & Co. KGaA, 2008), p. 1-116.

9. V.P. Parkhutik, J.M. Albella, Y.E. Makushok, I. Montero, J.M. Martinez-Duart, V.I. Shershulskii, *Electrochim. Acta* 35, 6 (1990): p. 955-960.

10. J.D. Venables, D.K. McNamara, J.M. Chen, T.S. Sun, R.L. Hopping, *Appl. Surf. Sci.* 3, 1 (1979): p. 88-98.

11. G.W. Critchlow, K.A. Yendall, D. Bahrani, A. Quinn, F. Andrews, *Int. J. Adhes. Adhes.* 26, 6 (2006): p. 419-453.

12. J.D. Venables, "27," in *Adhesion and Durability of Metal/Polymer Bonds*, ed. K.L. Mittal, ed.Springer US, 1984), p. 453-467.

13. A.J. Kinloch, M.S.G. Little, J.F. Watts, *Acta Mater.* 48, 18–19 (2000): p. 4543-4553.

14. G.D. Sulka, K.G. Parkoła, *Electrochim. Acta* 52, 5 (2007): p. 1880-1888.

15. G.D. Davis, P.L. Whisnant, J.D. Venables, *J. Adhes. Sci. Technol.* 9, 4 (1995): p. 433-442.

16. J. van den Brand, S.V. Gils, H. Terryn, V.G.M. Sivel, J.H.W.d. Wit, *Prog. Org. Coat.* 51, 4 (2004): p. 351-364.

17. J. van den Brand, S. Van Gils, P.C.J. Beentjes, H. Terryn, J.H.W. de Wit, *Appl. Surf. Sci.* 235, 4 (2004): p. 465-474.

18. J.A. Kelber, R.K. Brow, *Appl. Surf. Sci.* 59, 3–4 (1992): p. 273-280.

19. D. Mercier, J.C. Rouchaud, M.G. Barthés-Labrousse, *Appl. Surf. Sci.* 254, 20 (2008): p. 6495-6503.

20. C. Fauquet, P. Dubot, L. Minel, M.G. Barthés-Labrousse, M. Rei Vilar, M. Villatte, *Appl. Surf. Sci.* 81, 4 (1994): p. 435-441.

21. J. van den Brand, O. Blajiev, P.C.J. Beentjes, H. Terryn, J.H.W. de Wit, *Langmuir* 20, 15 (2004): p. 6318-6326.

22. Ö. Özkanat, F.M. de Wit, J.H.W. de Wit, H. Terryn, J.M.C. Mol, *Surf. Coat. Technol.* 215, 0 (2013): p. 260-265.

23. J.F. Watts, A. Rattana, M.-L. Abel, *Surf. Interface Anal.* 36, 11 (2004): p. 1449-1468.

24. S.T. Abrahami, T. Hauffman, J.M.M. de Kok, H. Terryn, J.M.C. Mol, *Surf. Interface Anal.* 48, 8 (2016): p. 712-720.

25. J. Marsh, L. Minel, M.G. Barthés-Labrousse, D. Gorse, *Appl. Surf. Sci.* 133, 4 (1998): p. 270-286.

26. S.T. Abrahami, T. Hauffman, J.M.M. de Kok, J.M.C. Mol, H. Terryn, *J. Phys. Chem. C* 120, 35 (2016): p. 19670-19677.

27. D. Packham, "2," in *Theories of Fundamental Adhesion*, ed. eds. L.M. da Silva, A. Öchsner , R. Adams, ed.Springer Berlin, 2011), p. 9-38.

28. M.-L. Abel, R.P. Digby, I.W. Fletcher, J.F. Watts, *Surf. Interface Anal.* 29, 2 (2000): p. 115-125.

29. M. Öhman, D. Persson, *Surf. Interface Anal.* 44, 2 (2012): p. 133-143.

30. C. Le Pen, B. Vuillemin, S. Van Gils, H. Terryn, R. Oltra, *Thin Solid Films* 483, 1–2 (2005): p. 66-73.

31. J. Kim, P.C. Wong, K.C. Wong, R.N.S. Sodhi, K.A.R. Mitchell, *Appl. Surf. Sci.* 253, 6 (2007): p. 3133-3143.

32. R.F. Wegman, J. Van Twisk, in *2 - Aluminum and Aluminum Alloys*, ed. eds. R.F. Wegman , J.V. Twisk, ed.William Andrew Publishing, 2013), p. 9-37.

33. A.M. Cabral, R.G. Duarte, M.F. Montemor, M.G.S. Ferreira, *Prog. Org. Coat.* 54, 4 (2005): p. 322-331.

34. J. Song, W.J. Van Ooij, *J. Adhes. Sci. Technol.* 17, 16 (2003): p. 2191-2221.

35. A. Franquet, H. Terryn, J. Vereecken, *Surf. Interface Anal.* 36, 8 (2004): p. 681-684.

36. J. van den Brand, W.G. Sloof, H. Terryn, J.H.W. de Wit, *Surf. Interface Anal.* 36, 1 (2004): p. 81-88.

37. P.G. Sheasby, R. Pinner, *Surface Treatment and Finishing of Aluminium and Its Alloys*, 6th ed.(England: Finishing Publications Ltd., 2001.).

38. A.V. Pocius, in The Chemistry and Physical Properties of Structural Adhesives, ed.Hanser, 2012), p. 219-258.

39. A.V. Pocius, in The Chemistry and Physical Properties of Elastomer-Based Adhesives, ed.Hanser, 2012), p. 273-306.

40. "Standard Test Method for Floating Roller Peel Resistance of Adhesives" (West Conshohocken, PA: ASTM International, 2003), p.

41. V.P. Parkhutik, V.T. Belov, M.A. Chernyckh, *Electrochim. Acta* 35, 6 (1990): p. 961-966.

42. M.R. Alexander, G.E. Thompson, G. Beamson, *Surf. Interface Anal.* 29, 7 (2000): p. 468-477.

43. E. McCafferty, J.P. Wightman, *Surf. Interface Anal.* 26, 8 (1998): p. 549-564.

44. W. Brockmann, O.D. Hennemann, H. Kollek, C. Matz, *Int. J. Adhes. Adhes.* 6, 3 (1986): p. 115.

45. R. Tannenbaum, S. King, J. Lecy, M. Tirrell, L. Potts, *Langmuir* 20, 11 (2004): p. 4507-4514.

46. S. Pletincx, L. Trotochaud, L.L. Fockaert, A.R. Head, O. Karshoglu, J.M.C. Mol, B. H., H. Terryn, T. Hauffman, *Scientific reports* in press, (2017):

47. T. Semoto, Y. Tsuji, K. Yoshizawa, *J. Phys. Chem. C* 115, 23 (2011): p. 11701-11708.

48. S. Ogata, Y. Takahashi, *J. Phys. Chem. C* 120, 25 (2016): p. 13630-13637.

49. R. Posner, O. Ozcan, G. Grundmeier, in *Water and Ions at Polymer/Metal Interfaces*, ed. eds. M.L.F. Silva , C. Sato, ed.(Berlin, Heidelberg: Springer Berlin Heidelberg, 2013), p. 21-52.

50. G. Kacar, E.A.J.F. Peters, L.G.J. van der Ven, G. de With, *PCCP* 17, 14 (2015): p. 8935-8944.

51. M. Mohseni, M. Mirabedini, M. Hashemi, G.E. Thompson, *Prog. Org. Coat.* 57, 4 (2006): p. 307-313.

52. M.-L. Abel, J.F. Watts, R.P. Digby, *Int. J. Adhes. Adhes.* 18, 3 (1998): p. 179-192.